Excited-State Forces within a First-Principles Green's Function Formalism

Sohrab Ismail-Beigi and Steven G. Louie
Department of Physics, University of California, Berkeley, California 94720
and Materials Sciences Division, Lawrence Berkeley National Laboratory, Berkeley, California 94720
(Received 11 July 2002; published 19 February 2003)

We present a new first-principles formalism for calculating forces for optically excited electronic states using the interacting Green's function approach with the *GW* Bethe-Salpeter-equation method. This advance allows for efficient computation of gradients of the excited-state Born-Oppenheimer energy, allowing for the study of relaxation, molecular dynamics, and photoluminescence of excited states. The approach is tested on photoexcited carbon dioxide and ammonia molecules, and the calculations accurately describe the excitation energies and photoinduced structural deformations.

DOI: 10.1103/PhysRevLett.90.076401 PACS numbers: 71.15.–m, 73.22.–f, 71.35.–y, 78.55.–m

Calculation of optically excited electronic states and spectra has recently become possible through use of the interacting two-particle Green's function within the first-principles *GW*-Bethe-Salpeter-equation (*GW*-BSE) formalism [1,2], making possible the study of photoinduced structural change and photoluminescence. However, within this methodology, one calculates optical properties at fixed ionic positions: Barring inefficient finite-difference schemes or shrewd guesses, the direction in the multidimensional space of ionic configurations best optimizing the geometry is unknown. The problem is of practical importance since structural changes due to optical excitation are general phenomena which cause atomic rearrangement or dissociation and change the structure or symmetry of defects. The possibility of efficient *ab initio* calculation of excited-state forces opens new doors to reliable study of such changes.

To this end, we present a new formalism for calculating excited-state forces within the *GW*-BSE approach. We develop the theory for the force calculations and the approximations requisite to render computations tractable and then carry out practical tests for two molecules. We also compare our results to those of constrained density functional theory (CDFT) [3]. Our development of force calculations parallels recent quantum chemistry advances (e.g., [4]) where analytical forces can be calculated for excited-state methods [CIS, CIS(D), EOM-CCSD]. These methods provide an overall accuracy similar to the *GW*-BSE method [4,5]. However, the *GW*-BSE method scales as N^4 (N is the number of atoms in the system), whereas these methods scale as N^6 or worse. In addition, quantum chemistry methods are much more difficult to apply to bulk solids whereas the *GW*-BSE method scales equally well in the bulk limit.

Within the *ab initio GW*-BSE approach, we obtain the ground-state electron density, total energy, forces, and single-particle states $|i\rangle^{\mathrm{DFT}}$ and eigenvalues $\varepsilon_i^{\mathrm{DFT}}$ using density functional theory (DFT) [6]. We then construct the RPA dielectric function ϵ^{-1} and the screened interaction $W = \epsilon^{-1} v_c$, where v_c is the Coulomb interaction $v_c(\vec{r}, \vec{r}') = 1/|\vec{r} - \vec{r}'|$. We find quasiparticle excitations by using the *GW* approximation to the self-energy, $\Sigma = iGW$ [7]. The effective quasiparticle Hamiltonian H^{qp} is

$$\hat{H}^{qp} = \hat{T} + \hat{V}_{sc} + (\hat{\Sigma} - \hat{V}_{xc}), \tag{1}$$

where T is the kinetic operator and $V_{sc} = V_{ion} + V_H + V_{xc}$ is the sum of the ionic, Hartree, and DFT mean-field exchange-correlation potentials. We solve the Dyson equation $\hat{H}^{qp}|i\rangle = \varepsilon_i|i\rangle$ to obtain quasiparticle energies ε_i and eigenstates $|i\rangle$.

Two-particle excited-state properties are obtained by solving the Bethe-Salpeter equation of the two-particle Green's function. We employ the "standard" positive-frequency version of the BSE eigenvalue equation and restrict to static screening [1,2]. The BSE eigenvalue equation is

$$\sum_{c'v'} H^{\mathrm{BSE}}_{cv,c'v'} A^S_{c'v'} = \Omega_S A^S_{cv}, \tag{2}$$

with

$$H^{\mathrm{BSE}}_{cv,c'v'} = (\varepsilon_c - \varepsilon_v)\delta_{cc'}\delta_{vv'} + K_{cv,c'v'}. \tag{3}$$

Here c labels unoccupied (conduction) states, v labels occupied (valence) states, A^S_{cv} is the electron-hole amplitude for a quasihole in state v and a quasielectron in state c, S labels an excited state, Ω_S is the excitation energy, and H^{BSE} is the effective electron-hole Hamiltonian. The excited-state energy is given by $E_S = E_0 + \Omega_S$, where E_0 is the ground-state energy. K is the electron-hole interaction kernel with matrix elements

$$K_{cv,c'v'} = \int c(1)^* v(2) \Xi(1234) c'(3) v'(4)^* \, d(1234), \tag{4}$$

where $j(1) = \langle 1|j\rangle$. The kernel Ξ is

$$\Xi(1234) = -\delta(13)\delta(24)W(12) + \delta(12)\delta(34)v_c(13). \tag{5}$$

The static screening approximation means that $W = \epsilon^{-1} v_c$ uses the static dielectric function $\epsilon^{-1}(\omega = 0)$ in Eq. (5). We note that the frequency dependent $\epsilon^{-1}(\omega)$ is

used in the GW quasiparticle calculations. We use the standard normalization $\sum_{cv} |A^S_{cv}|^2 = 1$.

Our aim is to compute excited-state forces, i.e., derivatives of E_S versus the $3N$ ionic coordinates R, denoted as $\partial_R E_S$. The derivatives have two parts:

$$\partial_R E_S = \partial_R E_0 + \partial_R \Omega_S.$$

DFT provides the ground-state derivatives $\partial_R E_0$ [6]. The BSE provides expressions for Ω_S, and we compute $\partial_R \Omega_S$ directly. Using Eq. (3) and the normalization condition for A^S_{cv}, we have

$$\partial_R \Omega_S = \sum_{cv,c'v'} A^{S*}_{cv} A^S_{c'v'} \partial_R H^{\mathrm{BSE}}_{cv,c'v'}, \tag{6}$$

where

$$\partial_R H^{\mathrm{BSE}}_{cv,c'v'} = (\partial_R \varepsilon_c - \partial_R \varepsilon_v)\delta_{cc'}\delta_{vv'} + \partial_R K_{cv,c'v'}. \tag{7}$$

The derivative $\partial_R H^{\mathrm{BSE}}$ contains two types of terms, those involving $\partial_R \varepsilon_i$ and those involving $\partial_R K$. Below, we adopt two physical approximations to render computations tractable.

Since $\hat{H}^{qp}|i\rangle = \varepsilon_i |i\rangle$ is a standard eigenvalue equation, standard first order perturbation theory yields

$$\begin{aligned} \partial_R \varepsilon_i &= \langle i|\partial_R \hat{H}^{qp}|i\rangle, \\ P^R_{ji} &\equiv \langle j|\{\partial_R|i\rangle\} \\ &= \left\{ \begin{array}{ll} 0 & \text{if } \varepsilon_i = \varepsilon_j \\ \frac{\langle j|\partial_R \hat{H}^{qp}|i\rangle}{\varepsilon_i - \varepsilon_j} & \text{if } \varepsilon_i \neq \varepsilon_j \end{array} \right\}. \end{aligned} \tag{8}$$

Evaluating $\partial_R \hat{H}^{qp} = \partial_R \hat{V}_{sc} + \partial_R(\hat{\Sigma} - \hat{V}_{xc})$ is burdensome as $\partial_R \hat{\Sigma}$ contains the derivatives $\partial_R G$ and $\partial_R \epsilon^{-1}$, both prohibitive to calculate. We choose a physical approximation: As discussed above, V_{sc} contains the dominant ionic, Hartree, and mean-field exchange-correlation potentials which bind solids and molecules. The weaker correction $\Sigma - V_{xc}$ consists largely of a constant "scissors-shift" with a weak dependence on R. Therefore, we approximate $\partial_R \hat{H}^{qp} \cong \partial_R \hat{V}_{sc}$. To calculate $\partial_R V_{sc}$, we employ density functional perturbation theory [8]: An auxiliary quadratic functional is minimized, and at its minimum $\partial_R V_{sc}$ is easily found. We perform $3N$ minimizations for the $3N$ choices of R.

Considering $\partial_R K$ and examining Eqs. (4) and (5), there are two distinct types of derivatives: those containing $\partial_R|i\rangle$ and those containing $\partial_R W$. For the first set, we employ Eq. (8) and sum over intermediate states to reach convergence. For the second set, we now argue (and numerically verify below) that they are negligible. Specifically, $W = \epsilon^{-1} v_c$ where $\epsilon = I - v_c P$ and P is the irreducible polarizability. Within the RPA approximation that we employ, $P = iGG$ is a function of G alone and thus so are ϵ and W, so the chain rule yields $\partial_R W(12) = \int \frac{\delta W(12)}{\delta G(34)} \partial_R G(34) d(34)$. In deriving the interaction kernel Ξ, we assume that $\delta W/\delta G \cong 0$ [2]. Judging from the success and accuracy of the BSE based on this assumption, we conclude that we may set $\partial_R W \cong 0$. Thus, we arrive at the following expression for $\partial_R K$:

$$\begin{aligned} \partial_R K_{cv,c'v'} = \sum_j [&P^{R*}_{jc} K_{jv,c'v'} + P^R_{jv} K_{cj,c'v'} \\ &+ P^R_{jc'} K_{cv,jv'} + P^{R*}_{jv'} K_{cv,c'j}]. \end{aligned} \tag{9}$$

Taken together, Eqs. (6)–(9) provide an explicit expression for $\partial_R \Omega_S$ and, hence, $\partial_R E_S$.

We now present test applications to verify the accuracy of our approach for molecules for which high quality excited-state observations are available. We begin by considering the first singlet excited-state of carbon monoxide (CO) which has one degree of freedom R.

We carry out DFT calculations using the plane-wave pseudopotential method within the local density approximation (LDA) [6]. We use Kleinmann-Bylander pseudopotentials with s and p projectors (p local) for C and O with cutoff radii of $r_c = 1.3$ a.u. [9] and expand the electronic states to a plane-wave cutoff of 70 Ry. Our periodic supercell is a $7 \times 7 \times 7$ Å^3 cube. We sample the Brillouin zone at $k = 0$. We perform GW calculations using the generalized plasmon-pole model [7]. We include 600 bands in the GW calculations to converge *absolute* quasiparticle and ionization energies. In the GW-BSE computations, we truncate the Coulomb interaction beyond 3.5 Å to avoid spurious periodic image interactions [2]. With these parameters, all reported energies are converged to 0.05 eV. For comparison, we also calculate excited-state properties with the constrained-LDA (CLDA) method: We occupy the lowest unoccupied molecular orbital (LUMO) with an electron taken from the highest occupied molecular orbital (HOMO) and iterate to self-consistency.

We mention two technical issues: (i) Off-diagonal matrix elements of H^{qp} in the DFT basis are required; their neglect changes Ω_S by $\sim \pm 0.2$ eV, as noted previously [10]; (ii) in the DFT supercell calculations, the Coulomb interaction has infinite range; this creates an ambiguity in the vacuum level and shifts quasiparticle energies by a constant. By varying the supercell volume V, we find the shift proportional to $1/V$ and extrapolate to $V \to \infty$.

Figure 1 displays the energy of the ground state and first singlet excited state of CO as a function of the bond length. Table I lists calculated and experimental properties of the ground state ($X^1\Sigma^+$) and excited state ($A^1\Pi$): equilibrium bond lengths R_e, harmonic vibration frequency ω_e, ionization energy IP (the HOMO energy for the LDA), and the minimum-to-minimum transition energy T_e. Results are also presented for representative quantum chemical methods for which forces have been developed. The ground-state LDA R_e and ω_e are in good agreement with experimental results, and the quantum chemical results are slightly superior due to the better treatment of correlation. While the LDA HOMO energy

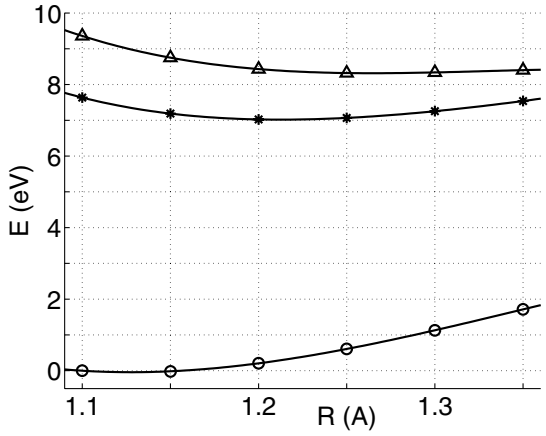

FIG. 1. $X^1\Sigma^+$ ground-state LDA (circles) and $A^1\Pi$ first excited-state energies (triangles are *GW*-BSE; stars are CLDA) versus the bond length R for CO. The continuous curves are polynomial fits.

lies far from the ionization energy, the *GW* results remove this error. The BSE results for the transition energy T_e to the excited state agree with experiment with an error typical of the method [2], whereas the CLDA transition energy is off by 1 eV. For R_e and ω_e, both the CLDA and BSE perform equally well; while we do not have an explanation for the size of the error, the fact that for this particular excitation the CLDA produces an ω_e of similar quality to the BSE one is explained by the observation (see below) that both methods produce similar variation of force versus bond length. The BSE results for T_e are of equal or better quality than the quantum chemical results, whereas for R_e and ω_e they are slightly worse.

Turning to the forces, we wish to know how accurately we can compute $\partial_R E_S$, i.e., the slope of the curves in Fig. 1. Figure 2 presents the calculated forces, as formulated above, along with "exact" forces obtained from two-point finite differences of the BSE energies. We also compute forces by assuming $\partial_R K = 0$ in Eq. (7), a quasiparticle-only treatment and the closest analogue to the single-particle CLDA. Both these single-particle methods predict equal and opposite forces for the C and O atoms, signaling that $\partial_R H^{qp} \cong \partial_R V_{sc}$ is a good approximation. Interestingly, both produce similar forces that depart from the exact forces by essentially a constant. Hence, both methods predict well the variation of the force versus R, an *a posteriori* verification of our physical intuition that changes in the mean-field potential V_{sc} dominate.

When we include contributions from $\partial_R K$, the forces improve markedly. Since we assume that $\partial_R W \cong 0$, the forces on C and O are no longer exactly equal and opposite. However, as Fig. 2 shows, the deviations are quite small on the relevant scale: As remarked above, the approximation $\partial_R W \cong 0$ is excellent in practice. If we subtract the unphysical net force on the center of mass (i.e., averaging the C and O values in Fig. 2), the calculated forces become essentially "exact."

CO has a single degree of freedom allowing for careful study. However, calculation of forces is truly useful when there are many degrees of freedom and one does not know, *a priori*, which are the relevant ones for a given excited state. We now consider the first singlet excited-state of ammonia, NH_3, a molecule with six degree of freedom. We employ identical methods as in the case of CO and provide key parameters: s projector for H ($r_c = 0.8$ a.u.); s and p projectors for N (p local, $r_c = 1.0$ a.u.); identical supercell, k points, and Coulomb truncation radius; a 50 Ry cutoff for the wave functions; 600 bands in the *GW* portion; all energies converged to 0.05 eV.

TABLE I. Ground-state and excited-state data for CO: equilibrium bond length R_e, harmonic vibrational frequency ω_e, ionization potential IP, and $X^1\Sigma^+ \rightarrow A^1\Pi$ minimum-to-minimum transition energy T_e.

	Ground state ($X^1\Sigma^+$)		
	R_e (Å)	ω_e (cm^{-1})	IP (eV)
LDA	1.13	2050	9.1
GW	···	···	14.1
MP2 [4]	1.133	2151	···
CCSD [4]	1.124	2243	···
Expt. [11]	1.128	2170	14.01
	Excited state ($A^1\Pi$)		
	R_e (Å)	ω_e (cm^{-1})	T_e (eV)
CLDA	1.21	1720	7.02
GW-BSE	1.26	1290	8.32
CIS [4]	1.21	1633	8.83
EOM-CCSD [4]	1.22	1593	7.91
Expt. [11]	1.24	1518	8.07

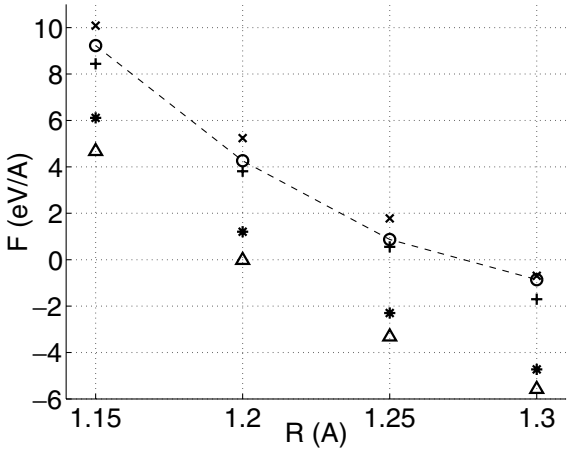

FIG. 2. Absolute magnitudes of $A^1\Pi$ excited-state forces for CO. Circles are "exact" *GW*-BSE forces. Crosses and plusses are calculated *GW*-BSE forces on C and O. Triangles are *GW*-BSE forces with $\partial_R K = 0$. Stars are CLDA forces. The dashed curve is a guide for the "exact" forces.

TABLE II. Ground-state and excited-state data for NH_3: equilibrium bond length R_e, H-N-H angle θ, ionization potential IP, and $\tilde{X}^1A_1 \rightarrow \tilde{A}^1A_2''$ transition energy T_e. The experimental T_e contains a zero-point contribution of unknown but presumably small size.

	Ground state ($\tilde{X}^1A_1$)		
	R_e (Å)	θ (°)	IP (eV)
LDA	1.03	105.0	6.2
GW	···	···	10.7
Expt. [11,12]	1.01	106.7	10.1
	Excited state ($\tilde{A}^1A_2''$)		
	R_e (Å)	θ (°)	T_e (eV)
CLDA	1.08	120	5.05
GW-BSE	1.08	120	5.52
CASSCF [13]	1.06	120	5.49
CEPA [13]	1.06	120	5.63
Expt. [12]	1.08	120	5.7

Table II lists properties of the LDA ground state. Starting with this ground state, for the BSE we consider the first singlet excited state, and for the CLDA we promote an electron from HOMO to LUMO. We compute excited-state forces and perform relaxations until bond lengths are converged to 0.01 Å, bond angles to 1°, and transition energies to 0.01 eV. Table II presents results for the relaxed excited state using CLDA, *GW*-BSE, and representative quantum chemical methods. The BSE excitation energy compares well with experimental and quantum chemical values. (The flattening of NH_3 is along the famous "umbrella" mode.)

Based on these two cases, we have verified the accuracy of the BSE method for calculation of excited-state energies and geometries. Our approach provides excited-state forces which are, to an excellent approximation, the derivatives of the BSE energies. Intriguingly, for these two cases, CDFT yields inferior excitation energies but predicts geometries of comparable quality to the BSE ones. While encouraging, there are a number of serious problems with wider use of CDFT. Use of CDFT is straightforward when the excited state is composed mainly of a single configuration: In the cases above, the HOMO-LUMO combination has probability above 90% in the excited state. However, for higher excited states or larger systems, we can have multiple configurations, something we cannot know without solving the BSE. Therefore, we believe that CDFT may be a useful guide in certain circumstances, but results thus obtained must be carefully tested by more sophisticated methods.

In brief, we present an *ab initio* formalism for calculating excited-state forces within the *GW*-BSE method as well as approximations allowing for computational tractability. We compute the photoexcited properties of molecules and verify the accuracy of (a) the *GW*-BSE formalism for describing the excited-state energies and structural relaxations, and (b) the forces as per our formalism. The calculations are as accurate as leading methods used in quantum chemistry (for which analytical force calculations are available) while scaling significantly better with system size and being easily applicable to the bulk.

This work was supported by NSF Grant No. DMR-0087088 and by the Office of Energy Research, Office of Basic Energy Sciences, Materials Science Division of the U.S. DOE Contract No. DE-AC03-76SF00098. Computer resources were provided by the DOE at the Lawrence Berkeley National Laboratory National Energy Research Scientific Computing Center and by the NSF National Partnership for Advanced Computational Infrastructure at the San Diego Supercomputing Center. This work was facilitated by the DOE Computational Materials Science Network.

[1] M. Rohlfing and S. G. Louie, Phys. Rev. Lett. **81**, 2312 (1998); S. Albrecht, L. Reining, R. Del Sole, and G. Onida, Phys. Rev. Lett. **80**, 4510 (1998); L. X. Benedict, E. L. Shirley, and R. B. Bohn, Phys. Rev. Lett. **80**, 4514 (1998).

[2] M. Rohlfing and S. G. Louie, Phys. Rev. B **62**, 4927 (2000); G. Onida, L. Reining, and A. Rubio, Rev. Mod. Phys. **74**, 601 (2002).

[3] F. Mauri and R. Car, Phys. Rev. Lett. **75**, 3166 (1995).

[4] J. F. Stanton, J. Gauss, N. Ishikawa, and M. Head-Gordon, J. Phys. Chem. **103**, 4160 (1995).

[5] K. W. Sattelmeyer, J. F. Stanton, J. Olsen, and J. Gauss, Chem. Phys. Lett. **347**, 499 (2001).

[6] M. C. Payne, M. P. Teter, D. C. Allan, T. A. Arias, and J. D. Joannopoulos, Rev. Mod. Phys. **64**, 1045 (1992), and references therein.

[7] M. S. Hybertsen and S. G. Louie, Phys. Rev. B **34**, 5390 (1986).

[8] X. Gonze, D. C. Allan, and M. P. Teter, Phys. Rev. Lett. **68**, 3603 (1992).

[9] L. Kleinman and D. M. Bylander, Phys. Rev. Lett. **48**, 1425 (1982).

[10] J. C. Grossman, M. Rohlfing, L. Mitas, S. G. Louie, and M. L. Cohen, Phys. Rev. Lett. **86**, 472 (2001).

[11] *NIST Chemistry WebBook, NIST Standard Reference Database #69*, edited by P. J. Linstrom and W. G. Mallard, 2001 (http://webbook.nist.gov).

[12] G. Herzberg, *Electronic Spectra and Electronic Structure of Polyatomic Molecules* (Krieger, New York, 1991).

[13] M. I. McCarthy, P. Rosums, H.-J. Werner, P. Botschwina, and V. Vaida, J. Chem. Phys. **86**, 6693 (1987).